Elsevier Editorial System(tm) for Intermetallics
Manuscript Draft

Manuscript Number:

Title: Phase separation in Ni70Nb30-xYx glasses

Article Type: BMG VII

Keywords: A.ternary alloy systems; B. thermal properties; C.rapid solidificationglass; F.diffraction

Corresponding Author: Dr. Norbert Mattern,

Corresponding Author's Institution: IFW Dresden

First Author: Norbert Mattern

Order of Authors: Norbert Mattern; Ulla Vainio, Dr.; Bjorn Schwarz, Dr.; Jin Man Park, Dr.; Do Hyang Kim, Prof.; Jurgen Eckert, Prof.

Abstract: Phase separated metallic glasses were prepared in the ternary Ni-Nb-Y system by rapid quenching of the melt. For Ni-rich alloys, early stage of spinodal decomposition or an almost homogeneous glassy state is obtained due to the reduction of the critical temperature of liquid-liquid phase separation near to the glass transition temperature. In situ small-angle X-ray scattering at elevated temperature gives evidence of on-going phase separation of the glass prior to crystallisation. The structural changes during isothermal heat treatment point to a spinodal mechanism of the decomposition. For glass with low Y-content (5 at %) no indication of phase separation is found in accordance with the composition dependence of the metastable miscibility gap of the supercooled liquid. Upon heating, the phase separated glass becomes a precursor and causes the nanostructure of the Ni2Y-phase formed as the first stage of crystallization.

Suggested Reviewers: Livio Battezzati Prof.
University Torino/Italy
livio.battezzati@unito.it
Expert on thermodynamics

E.S. Park Prof.
Seuol National University
espark@snu.ac.kr
published papers on phase separation of metallic glasses

Cover Letter

Leibniz Gemeinschaft

IFW Dresden e. V. • Postfach 27 01 16 • 01171 Dresden

Leibniz-Institut
für Festkörper- und
Werkstoffforschung
Dresden

Institut für Komplexe Materialien (IKM)

Dr. Norbert Mattern
Abteilungsleiter Strukturforschung

Tel: + 49 351 4659-367
Fax: + 49 351 4659-452
E-Mail: n.mattern@ifw-dresden.de

16. November 2009

Prof. D.H.. Kim

Intermetallics
Special issue
Editor BMG VII

Dear Prof Kim,

Enclosed I send you our contribution of the BMG VII conference

„Phase separation in $Ni_{70}Nb_{30-x}Y_x$ glasses“

by

N. Mattern, U.Vainio, B.Schwarz, J.M. Park[1], D.H. Kim and J. Eckert,

to be published in Intermetallics.

Scincerey Yours

Norbert Mattern

Phase separation in $Ni_{70}Nb_{30-x}Y_x$ glasses

N. Mattern[1,*], U.Vainio[2], B.Schwarz[1], J.M. Park[1,3], D.H. Kim[3], J. Eckert[1,4]

[1]IFW Dresden, Institute for Complex Materials, P.O. Box 270116, D-01171 Dresden, Germany
[2]HASYLAB at DESY, Notkestr. 85, D-22603 Hamburg, Germany
[3]Center for Non-crystalline Materials, Department of Metallurgical Engineering, Yonsei University, Seoul, Republic of Korea
[4]TU Dresden, Institute of Materials Science, D-01062 Dresden, Germany

Abstract

Phase separated metallic glasses were prepared in the ternary Ni-Nb-Y system by rapid quenching of the melt. For Ni-rich alloys, early stage of spinodal decomposition or an almost homogeneous glassy state is obtained due to the reduction of the critical temperature of liquid-liquid phase separation near to the glass transition temperature. In situ small-angle X-ray scattering at elevated temperature gives evidence of on-going phase separation of the glass prior to crystallisation. The structural changes during isothermal heat treatment point to a spinodal mechanism of the decomposition. For glass with low Y-content (5 at %) no indication of phase separation is found in accordance with the composition dependence of the metastable miscibility gap of the supercooled liquid. Upon heating, the phase separated glass becomes a precursor and causes the nanostructure of the Ni_2Y-phase formed as the first stage of crystallization.

Keywords: A.ternary alloy systems; B. thermal properties; C. rapid solidificationglass; F. diffraction;

[*]) Corresponding author. tel.:+49 351 4659 367: fax: +49 351 4659 452

e-mail address: n.mattern@ifw-dresden.de

1. Introduction

Decomposition and phase separation in the liquid occur in several binary alloy systems due to large positive enthalpy of mixing between elements like Nb-Y, Al-In, and Pb-Al [1]. For binary systems having a small value like Co-Cu [2] and Fe-Cu [3], a miscibility gap exists in the metastable undercooled liquid below the liquidus temperature. In bulk metallic glass forming alloys the addition of elements with strong positive enthalpy leads to improvement of ductility [4] or glass forming ability [5] in a certain composition range. Phase separated metallic glasses have been prepared in several alloy systems by rapid quenching the melt : Zr-Y-Al-Ni [6], Zr-La-Al-Ni-Cu [7], Zr-Y-Co-Al [8], Ni-Nb-Y [9], Zr-Nd-Al-Co [10] , Cu-(Zr,Hf)-(Gd,Y)-Al [11], and Zr-(Ce,Pr,Nd)-Al-Ni [12]. The phase separation of the liquid is determined by the thermodynamic properties of the alloy system. For the phase separated metallic glasses reported in [6-12] the critical temperature of liquid-liquid phase separation T_c is above the liquidus temperature. In this case, phase separation leads to a special microstructure with a length scale up to several microns and some self-similar features are observed by transmission electron microscopy [6, 13, 14]. The materials represent frozen-in late states which have passed decomposition and growth of the melts by diffusion and coalescence as well as secondary precipitations reactions.

Recently, we could prepare phase separated glasses in the Ni-Nb-Y system with fluctuation length in the nanometre range [15]. With increasing Ni-content the critical temperature T_C becomes lowered near to the glass transition temperature which enables freezing in the early stages of decomposition. In this paper, we report the influence of the yttrium content on the formation and transformation of early stages of phase separation in $Ni_{70}Nb_{30-x}Y_x$ glasses. In-situ small-angle X-ray scattering at elevated temperatures was applied in combination with simultaneous X-ray diffraction in order to analyse the temperature and time dependence of the decomposition. With regard to bulk metallic glasses

the question viewed is to which extend phase separation occurs if the concentration of the element responsible for phase separation becomes low.

2. Experimental

Pre-alloyed ingots were prepared by arc-melting elemental Ni, Nb and Y with purities of 99.9 % or higher in a Ti-gettered argon atmosphere. To ensure homogeneity, the samples were remelted several times. From these pre-alloys, thin ribbons (3 mm in width and 30 μm in thickness) with nominal compositions $Ni_{70}Nb_{15}Y_{15}$, $Ni_{70}Nb_{20}Y_{10}$, and $Ni_{70}Nb_{25}Y_5$ were prepared by single-roller melt spinning under argon atmosphere. The casting temperature was 1923 K. X-ray diffraction (XRD) patterns were recorded in Bragg-Brentano geometry with CoKα radiation using a Panalytical X'Pert Pro diffractometer. Differential scanning calorimetry (DSC) experiments were performed employing a Netzsch DSC 404 calorimeter with a heating rate of 20 K/min. Small angle X-ray scattering (SAXS) was measured at the B1 synchrotron beam line of HASYLAB/DESY using an energy of 16516 eV. Samples were mounted on a heating stage which was used under vacuum for in-situ measurements. Intensity curves were registered by a PILATUS 300k area detector at a distance covering a q-range between 0.2 and 4.3 nm^{-1}. The temperature was stepwise increased. For each temperature background was measured followed by a calibration standard (glassy carbon) and subsequent measurement of the sample. For isothermal analysis the samples were heated with 100 K/min up to the corresponding temperature and measurements were immediately started (5 min or 15 min per pattern) and repeated up to 10 hours. Simultaneously the wide-angle X-ray Scattering (WAXS) was recorded by a linear position sensitive detector (MYTHEN).

3. Results

The XRD patterns of as-quenched $Ni_{70}Nb_{15}Y_{15}$ ribbons are shown in Figure 1. The diffuse character of the scattering curves for all the as-quenched samples indicates the amorphous state. The amorphous structures were also confirmed by high resolution TEM, local electron diffraction, and DSC. TEM images of $Ni_{70}Nb_{15}Y_{15}$ glass exhibit a "homogeneous" microstructure [14, 15]. Figure 2 shows the thermal behaviour of the glasses by the corresponding DSC scans. Two crystallization events are visible for the $Ni_{70}Nb_{15}Y_{15}$ and $Ni_{70}Nb_{20}Y_{10}$ glasses. XRD measurements of samples heated in the DSC up to the characteristic temperatures identify the first exothermal event as crystallization of a Ni_2Y nano phase (about 5 nm in size indicated by broadened reflections, also confirmed by TEM [14]), and the second peak as the crystallization of $NbNi_3$ respectively. Simultaneously with the formation of $NbNi_3$ the reflections of Ni_2Y become sharp indicating the growth of the former nanocrystals. In contrast, the $Ni_{70}Nb_{25}Y_5$ glass exhibits only one single exothermal event corresponding to a eutectic crystallization of the amorphous phase into Ni_2Y+$NbNi_3$. In order to analyse the homogeneity of the $Ni_{70}Nb_{30-x}Y_x$ glasses, SAXS was measured at different temperatures. Especially the simultaneous registration of WAXS patterns should reveal whether phase separation occurs before crystallization. SAXS provides integral information on existing inhomogeneities in electron density with a size ranging from the nanometre up to the micron range. The calibrated small angle X-ray scattering curves depend on differences in electron density, but also on the volume fraction, size, and shape of the inhomogeneities built up from the different phases [16]:

$$\frac{d\sigma}{d\Omega}(q) = \int 4\pi \cdot r^2 \tilde{\eta}^2(r) \frac{\sin(qr)}{qr} dr \,, \qquad (1)$$

Where $d\sigma/d\Omega(q)$ is the differential cross section , q is the magnitude of the scattering vector ($q = 4\pi\sin\theta/\lambda$, scattering angle 2θ, wavelength λ), $\tilde{\eta}^2(r) = \tilde{\rho}(r)^2 - V\rho_0^{\,2}$ is the square of the so-

called electron density fluctuation, which is given by the difference of the electron scattering-length density $\rho(r)$ and the average electron scattering-length density ρ_0 in the sample volume V. Figures 3,4 show the obtained SAXS curves for two of the $Ni_{70}Nb_{30-x}Y_x$ glasses at elevated temperatures. The simultaneously measured WAXS patterns are also given by the insets. The as-cast states are characterized by a very weak SAXS intensity pointing to an almost homogeneous structure. The intensity increase below $q < 0.8$ nm^{-1} probably originates from surface scattering. With rising temperatures a pronounced maximum becomes evident for the $Ni_{70}Nb_{15}Y_{15}$ glass, and it increases in height and shifts in position to lower q-values. Such a maximum is an indication of a dominant correlation length. Using the relationship $\zeta = 2\pi/q_{max}$ between correlation length ζ and position of the maximum one obtains values of ζ between 5 and 10 nm. From the comparison with the XRD data it follows that the crystallization of the nanocrystalline Ni_2Y phase is clearly reflected by the SAXS data. The shift of the interference maximum to lower q-values indicates growth which is also seen by reduction of the width of reflection in the XRD patterns. The $Ni_{70}Nb_{20}Y_{10}$ glass shows a similar development of the SAXS patterns with temperature. However, for the $Ni_{70}Nb_{25}Y_5$ glass we observe a different behaviour. No change of the SAXS intensity (Fig. 4) is observed below crystallization temperature. First, the eutectic crystallization of the amorphous phase at T_x=823 K leads to a heterogeneous microstructure and to the increase of SAXS intensity. Figure 5 compares the temperature dependence of the integral (sum) of the SAXS intensities between q=0.2 and 3.0 nm^{-1} for the different glasses. For the $Ni_{70}Nb_{15}Y_{15}$ and $Ni_{70}Nb_{20}Y_{10}$ glasses an increase of the SAXS intensities is observed well below the crystallization temperature. The beginning crystallization is expressed by change of the slope of SAXS vs. T curves. Obviously for the $Ni_{70}Nb_{15}Y_{15}$ and $Ni_{70}Nb_{20}Y_{10}$ glasses phase separation occurs before crystallization. On the other side, for the $Ni_{70}Nb_{25}Y_5$ glass no indication of phase separation in the amorphous phase can be detected in the SAXS measurements. To analyze the time dependence of the decomposition, isothermal measurements of $Ni_{70}Nb_{15}Y_{15}$ and

$Ni_{70}Nb_{20}Y_{10}$ glasses were made at different temperatures. Figure 6 shows the SAXS measurements of $Ni_{70}Nb_{20}Y_{10}$ glass at T=753 K versus time. The WAXS patterns at the beginning and after a characteristic time, as well as the difference curve are presented by the inset in Fig. 6. The SAXS intensity increases during isothermal annealing of $Ni_{70}Nb_{20}Y_{10}$ glass at T=753 K indicating the ongoing phase separation. The WAXS curve does not change as can be seen by the difference curve $\Delta I = I_{t=360min} - I_{t=min}$. For $Ni_{70}Nb_{20}Y_{10}$ glass at T= 773K the beginning formation of the Ni_2Y phase is distinctly visible in the XRD pattern already after 10 min. Figure 7 compares the behaviour of the height $I(q_{max})$ and the position q_{max} of the SAXS intensity maximum versus time. For temperatures below the crystallization (T ≤753K) the integrated intensity increases and becomes saturated for longer annealing time. For temperature above the crystallization temperature (T≥773K) a much faster and stronger increase is observed due to the crystallization. The different mechanisms can clearly be distinguished by the way the interference maximum at q_{max} changes its position with time, staying constant for annealing below crystallization, but decreases with crystallization.

4. Discussion

In order to understand the structure formation of the rapidly quenched alloys one has to analyze the phase diagram. In the ternary Ni-Nb-Y system a miscibility gap exist in the equilibrium melt ranging from the binary Nb-Y liquid up to about 60 at.% Ni [17]. For higher Ni-content the critical temperature T_C decreases below the liquidus temperature resulting in a metastable miscibility gap. Figure 8 shows a pseudo-binary section of the ternary Ni-Nb-Y phase diagram calculated by the CALPHAD method using the thermodynamic description given in [17]. The bimodal curve is also depicted. The critical temperature of liquid-liquid phase

separation T_C is rather low and only slightly different from the glass transition temperature T_g. From this picture it is understandable that during rapid quenching early stages of spinodal decomposition or even an almost homogeneous glass can be frozen in if crystallization is avoided. Annealing the glass afterwards at elevated temperatures below the crystallization temperature leads to phase separation by nucleation and growth or by spinodal mechanisms or further development of already frozen in fluctuations [18, 19]. The spinodal decomposition is initiated via the spontaneous formation and subsequent growth of coherent composition fluctuations. In the experimental SAXS data (Fig. 7), the position of the maximum of $I(q)$ does not change below crystallisation. This means that for the $Ni_{70}Nb_{15}Y_{15}$ glass the fluctuation length remains constant and the amplitude of the fluctuation increases during the decomposition process. This behaviour points to spinodal decomposition mechanism in Ni-Nb-Y glasses. On the other hand crystallization is accompanied by nucleation and growth which is related to the shift of the maximum position q_{max} (Fig. 7). The continuous transition in the SAXS data demonstrates that the phase separated glass acts as a precursor for the nanocrystallisation. Due to the ongoing decomposition, the Y-content increases in the Y-enriched amorphous Ni-Y(Nb) phase. The crystallization temperature of the Ni-Nb-Y glass decreases with Y-content (Fig.2). So nucleation of Ni_2Y probably starts from the composition fluctuations with highest Y-content leading to a nanocrystalline microstructure as the first crystallization step.

5. Conclusions

Phase separated metallic glasses can be prepared in the ternary Ni-Nb-Y system by rapid quenching of the melt. The microstructure formed is essentially determined by the critical temperature T_C of liquid-liquid phase separation which is a function of the chemical

composition of the alloy. Almost homogeneous glassy state or early stages of spinodal decomposition are obtained if T_C is near to the glass transition temperature. Small-angle X-ray scattering is a powerful tool for detecting fluctuations in the nanometre range. Especially by in-situ measurements at elevated temperature evidence of phase separation prior to crystallisation was observed and from the time dependence of structural parameters during isothermal heat treatment a spinodal decomposition mechanism is concluded. Phase separation acts as a precursor for the nanocrystallization. For the low Y-content complete solubility is found in agreement with the composition dependence of the miscibility gap.

Acknowledgement

The authors thank M. Frey, S. Donath, and B. Opitz for sample preparation. Financial support of the Deutsche Forschungsgemeinschaft DFG (project Ma1531/10) is gratefully acknowledged.

References

[1] T.B. Massalski, Binary Alloy Phase Diagrams, ASM International, 1990.

[2] Y. Nakagawa, Acta Metall. 6 (1958) 704.

[3] S.P.Elder SP, A. Munitz , G.J. Abbaschian, Mater. Sci. Forum 50 (1989) 137.

[4] E.S. Park, D.H. Kim, Acta Mater. 54 (2006) 2597.

[5] D. X.u, G. Duan, W. L. Johnson, Phys Rev Lett. 92 (2004) 245504.

[6] A. Inoue , S. Chen,T. Masumoto, Mater. Sci. Eng., A179/180 (1994) 346.

[7] A.A.Kündig, M. Ohnuma, D.H. Ping, T. Ohkubo, K. Hono, Acta Mater.52 (2004) 2441.

[8] B.J. Park, H.J. Chang, D.H. Kim, W.T. Kim, Appl. Phys. Lett. 85 (2004)6353.

[9] Mattern N, Kühn U, Gebert A, Gemming T, Zinkevich M, Wendrock H, Schultz L, Scripta Mater. 53 (2005) 271.

[10] E.S. Park, E.Y. Jeong, J.K. Lee, A.R Kwon, A. Gebert, L. Schultz, H.J.Chang, D.H. Kim, Scripta Mater. 56 (2007)197.

[11] E.S. Park, J.S. Kyeong, D.H. Kim, Scripta Mater. 57 (2007) 49.

[12] T.Wada,, D.Louzguine-Luzgin, A. Inoue, Scripta Mater. 57 (2007) 901.

[13] B.J. Park, H.J. Chang, D.H. Kim, W.T. Kim WT, K. Chattopadhyay, T.A. Abindanan , S. Bhattacharyya, Phys.Rev. Lett. 6 (2006) 245503.

[14] N. Mattern, T. Gemming, G. Goerigk, J. Eckert, Scripta Mater. 57 (2007) 29.

[15] N. Mattern , G. Goerigk , U. Vainio, M.K. Miller, T. Gemming, J. Eckert, Acta Mater. 57 (2009) 903.

[16] O.Glatter, O. Kratky , Small-Angle X-ray Scattering, Academic Press, London, 1982.

[17] N. Mattern, M. Zinkevich, W. Löser, G. Behr, J. Acker, J. Phase Equil.& Diff. 29 (2008) 141.

[18] J.W. Cahn, J.E. Hillard , J. Chem. Phys. 31 (1959) 688.

[19] K.Binder, P.Fratzl, in: G. Kostorz (ed.), Phase Transformations in Material, Wiley-VHC , Weinheim, 2001; pp.409.

Figure Captions:

Fig. 1: XRD patterns of rapidly quenched $Ni_{70}Nb_{30-x}Y_x$ alloys (x= 5, 10, 15 at%)

Fig. 2: DSC scans 20K/min of rapidly quenched $Ni_{70}Nb_{30-x}Y_x$ alloys (x=5, 10, 15 at%)

Fig. 3: In-situ SAXS and WAXS (inset) at different temperatures for glassy $Ni_{70}Nb_{15}Y_{15}$

Fig. 4: In-situ SAXS and WAXS (inset) at different temperatures for glassy $Ni_{70}Nb_{25}Y_5$

Fig. 5: SAXS intensity of $Ni_{70}Nb_{30-x}Y_x$ glasses (x=5, 10, 15 at%) versus temperature during step-wise heating

Fig. 6: In situ SAXS and WAXS (inset) of glassy $Ni_{70}Nb_{20}Y_{10}$ at T=753K versus time

Fig. 7: Intensity and position q_{max} of SAXS maximum of glassy $Ni_{70}Nb_{30-x}Y_x$ versus time

Fig. 8: Pseudo-binary section of $Ni_{70}Nb_{30-x}Y_x$ phase diagram

Figure 1

Click here to download high resolution image

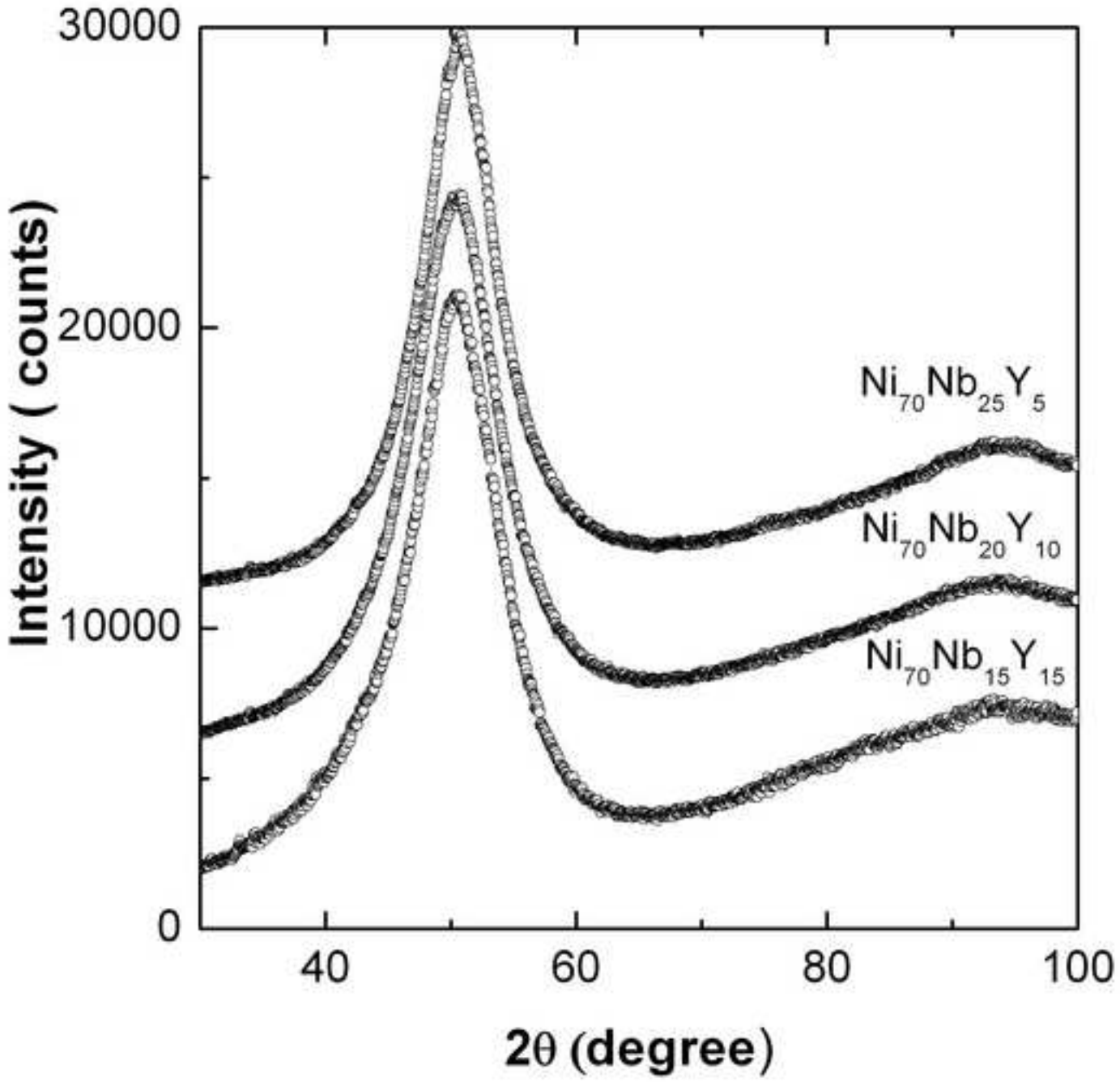

Figure 2

Click here to download high resolution image

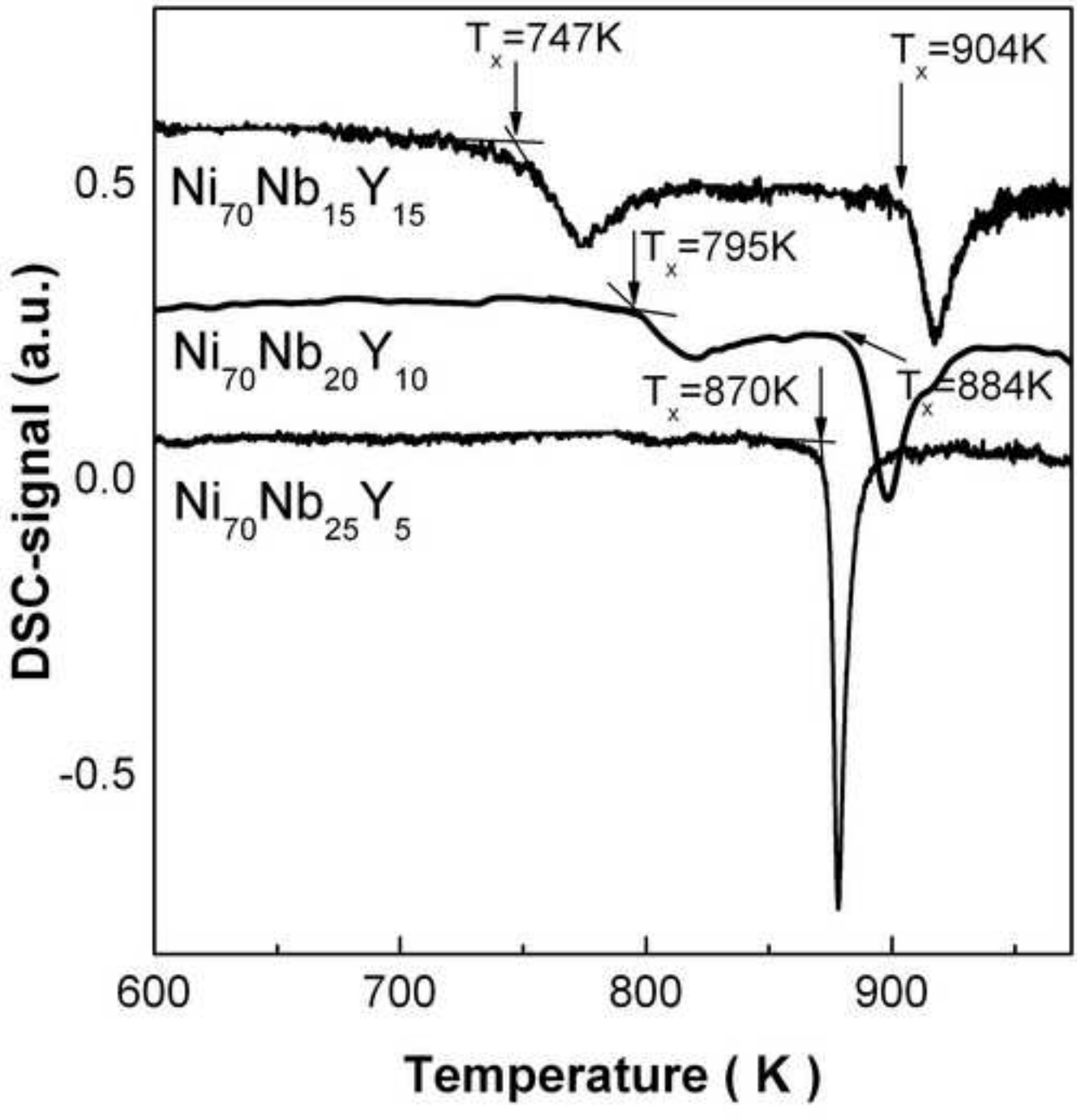

Figure 3

Click here to download high resolution image

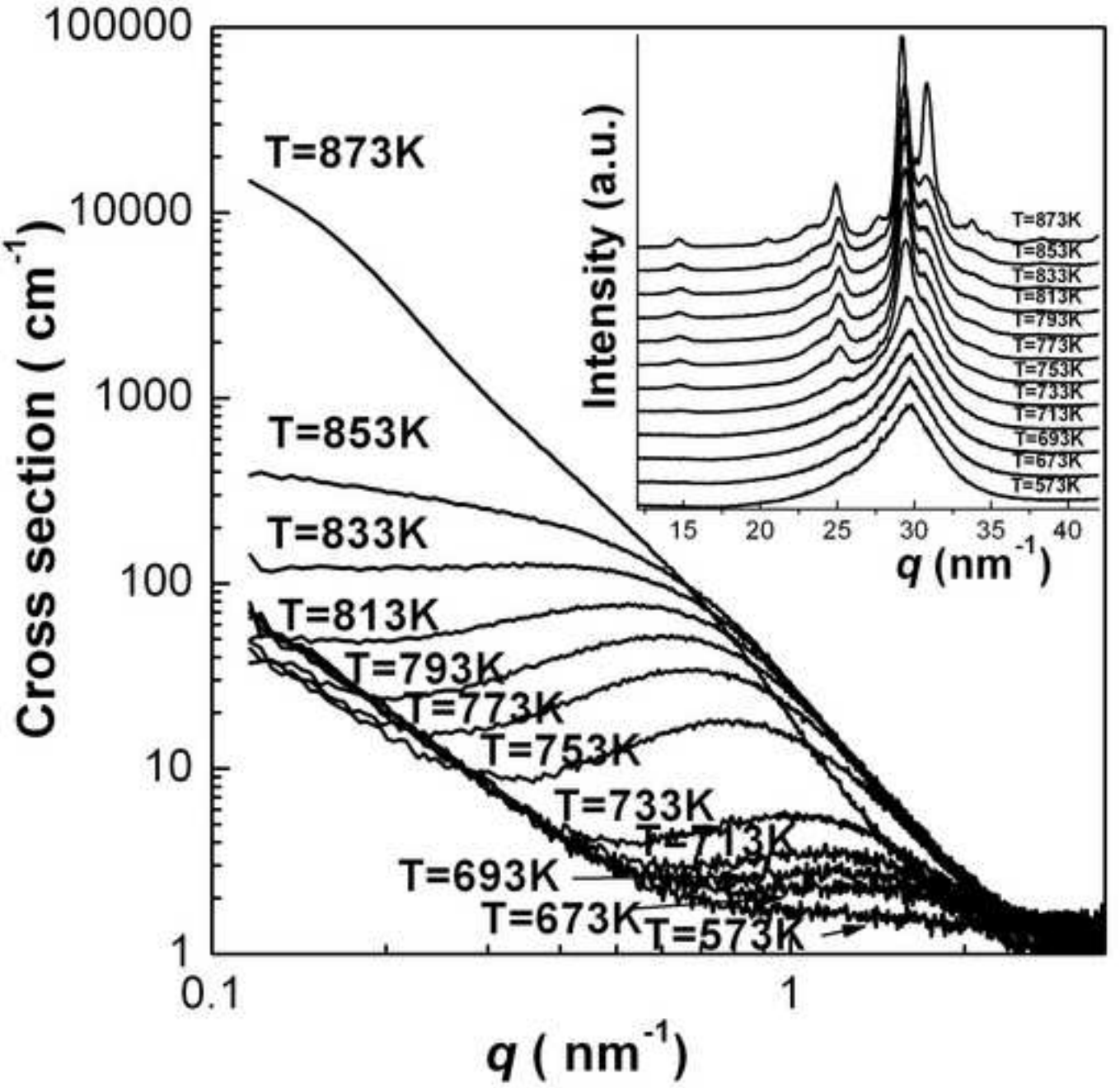

Figure 4

Click here to download high resolution image

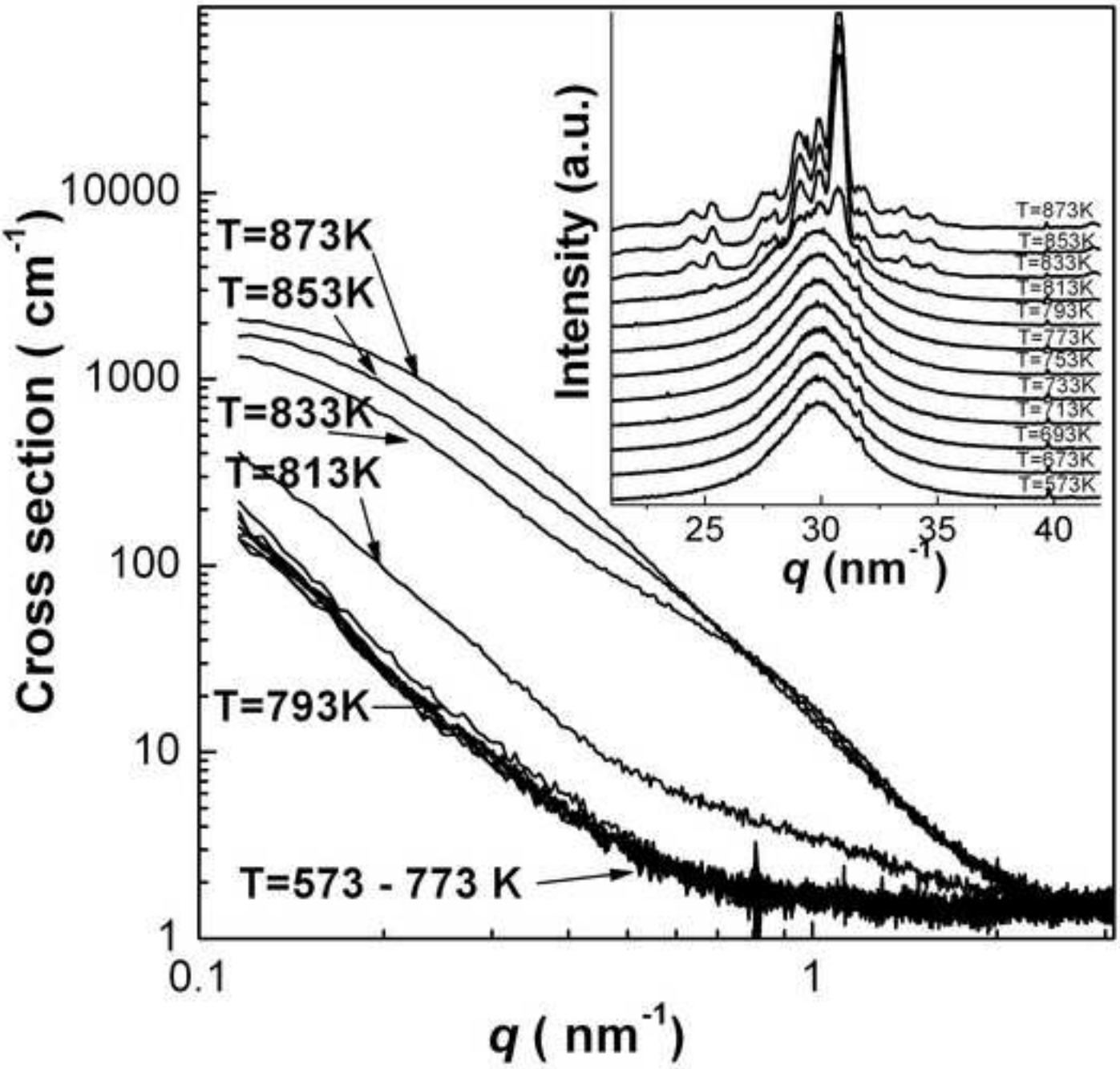

Figure 5

Click here to download high resolution image

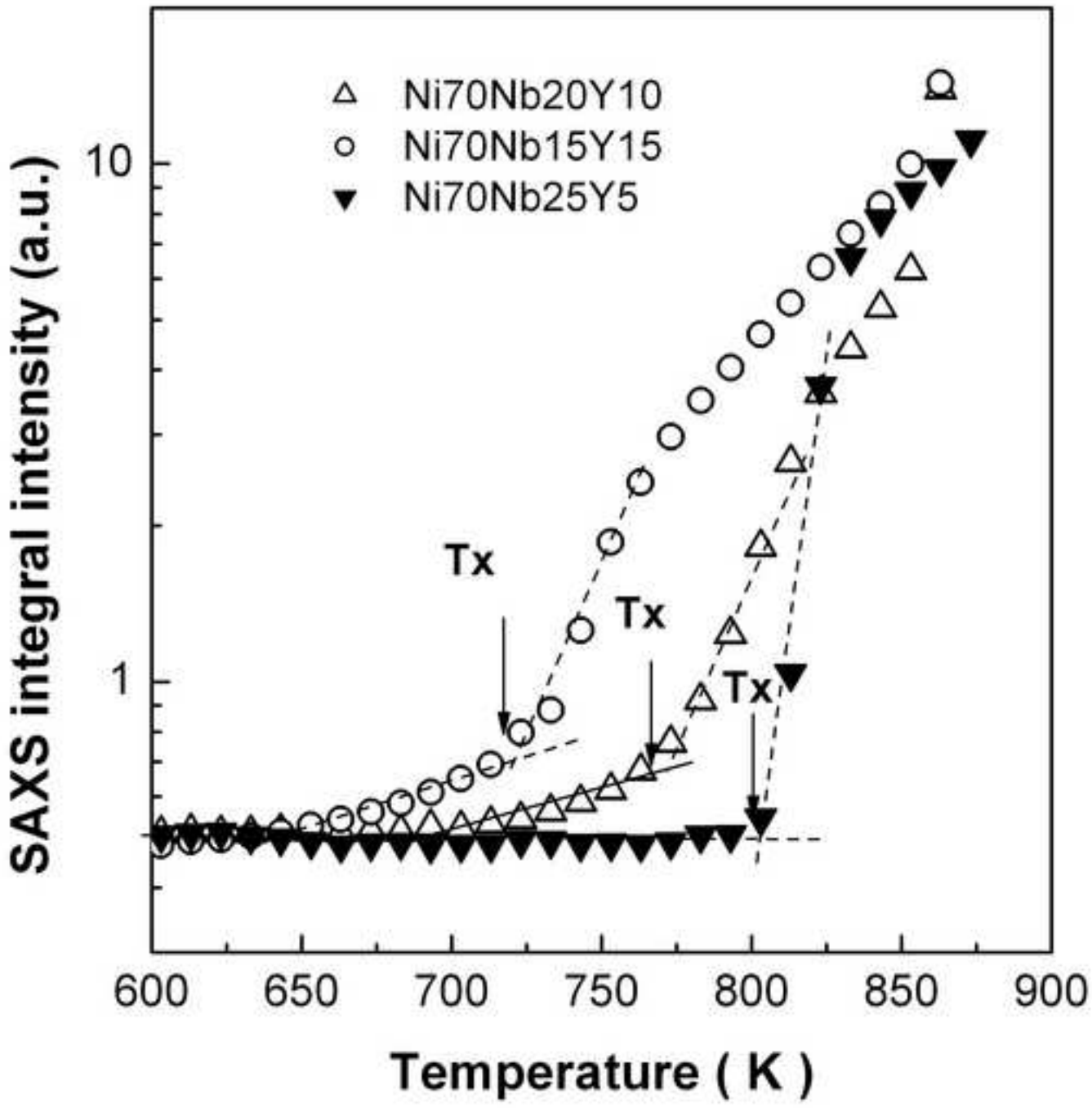

Figure 6

Click here to download high resolution image

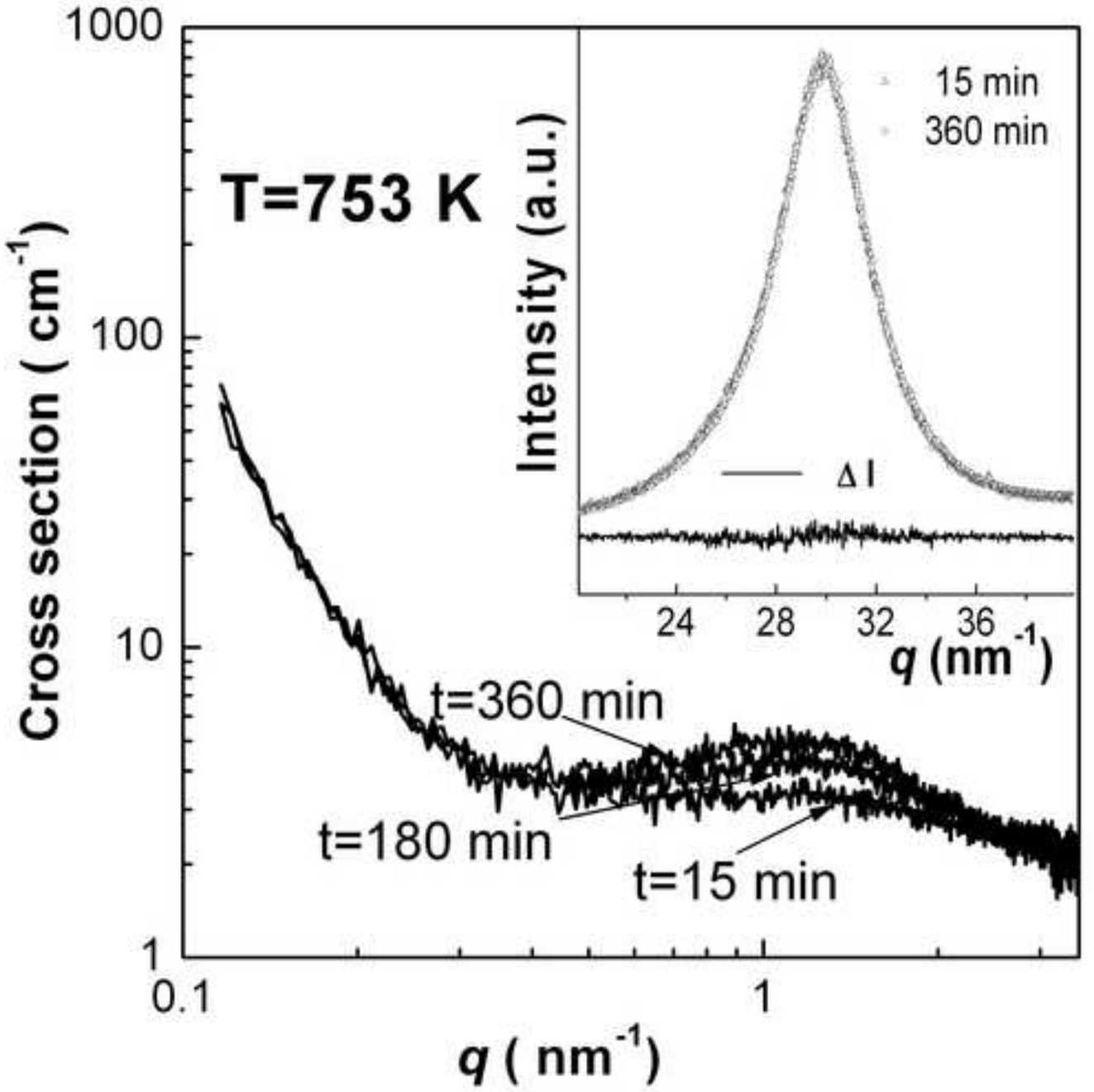

Figure 7

Click here to download high resolution image

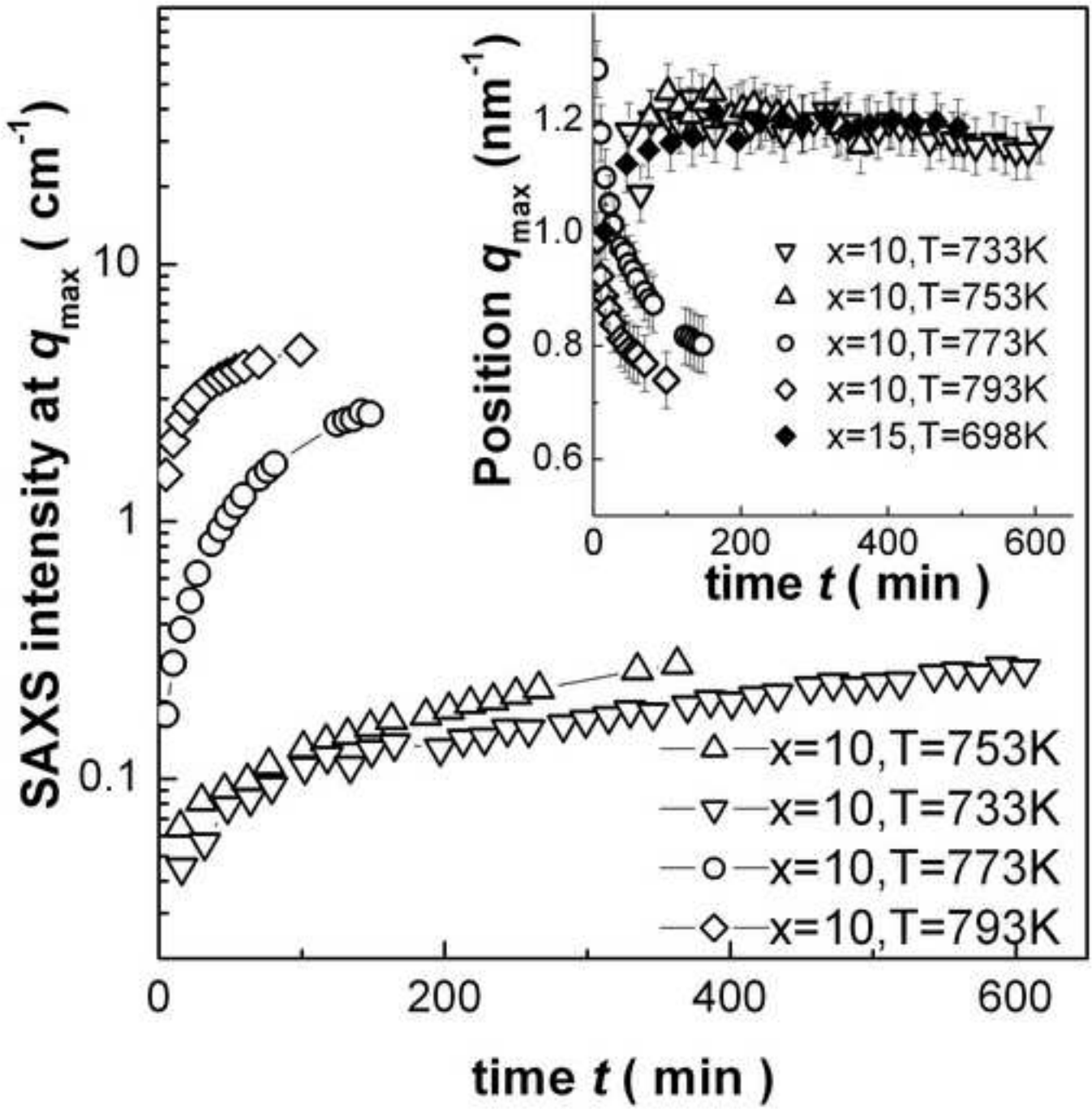

Figure 8

Click here to download high resolution image